

Environment-Insensitive Loop-type Antenna for Reliable Implant-to-Implant Communication

Abdul Basir
*Faculty of Information Technology
 and Communication Sciences
 Tampere University
 Tampere, Finland
 abdul.basir@tuni.fi*

Baqir Kazmi
*Faculty of Information Technology
 and Communication Sciences
 Tampere University
 Tampere, Finland
 baqir.kazmi@tuni.fi*

Uzman Ali
*Faculty of Information Technology
 and Communication Sciences
 Tampere University
 Tampere, Finland
 uzman.ali@tuni.fi*

Toni Björninen
*Faculty of Information Technology
 and Communication Sciences
 Tampere University
 Tampere, Finland
 toni.bjorninen@tuni.fi*

Abstract—Easy optimization, appropriate efficiency, and robustness are the key challenges in implantable antennas’ research. This paper presents the scalability analysis of a modified loop antenna, which shows insensitive behavior to implantation depth and variant dielectric environment. The proposed structure is optimized at two frequencies: 915 MHz and 2450 MHz. The antennas achieved fractional bandwidths of 3.1% and 15%, peak gains of -24.2 and -24.0 dBi, and radiation efficiencies of -30.1 and -30.3 dB. These characteristics together with the small geometry make the modified loop structure a suitable candidate for implant-to-implant communication.

Index Terms—Beam-width, environment-resilient, I2I communication, implantable devices, loop antenna.

I. INTRODUCTION

Recent advancements in implantable medical technologies have revolutionized healthcare and significantly enhanced the quality of life for patients with their astonishing abilities of diagnosis, monitoring, and treatment. Among these, implantable medical devices (IMDs) have gained significant attention. Conventional IMDs were able to do single tasks independently, such as stimulating or monitoring only one organ or drug delivery [1]. However, the introduction to implant-to-implant (I2I) communication makes them multi-tasking and ensures reliable communication to enhance IMDs’ functions through their mutual coordination.

However, the implementation of I2I communication presents significant challenges, including ensuring wireless accessibility, reliable communication, compactness in size, cost-effective production, and maintaining streamlined functionality despite the lossy and heterogeneous environment of the human body. Being the front-end component, these challenges are driven by the antenna due to its constrained properties inside the human body. The resonance frequencies and radiation properties

All authors were funded by Emil Aaltonen Foundation and the Research Council of Finland (funding decision: 349422).

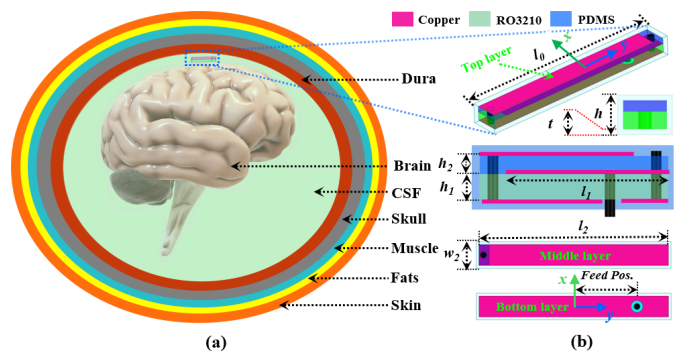


Fig. 1. Simulation setup and geometry of the proposed antenna. (a) Seven-layered head phantom where optimization of the antennas is carried out. (b) Detailed geometry of the proposed antenna.

of the implantable antennas are controlled by the dielectric properties (permittivity and conductivity) of the surrounding tissues, layered composition, curvature of the body-to-air interface, and implantation depth. Few studies in the past have overcome the frequency detuning in implantable antennas due to permittivity change by achieving wideband characteristics; however, all these antennas dramatically change the pattern and peak values of the gain when the implantation site or depth is changed. More specifically, the peak gain values of these antennas decrease with the increase in implantation depth and the pattern’s direction is towards the minimum tissue-to-air interface. To overcome the constraints above, this paper generalized the optimization of efficiency and environment-unaffected antennas for 915 MHz and 2450 MHz industrial, scientific, and medical band operations for I2I communication in the human head. The proposed antenna has fractional bandwidths of 3.1% and 15%; peak gains of -24.2 and -24.0 dBi; and radiation efficiencies of -30.1 and -30.3 dB at 915

TABLE I
DETAILED GEOMETRIC PARAMETERS OF THE ANTENNAS

Parameters (mm)	l_o	h_1	h_2	l_2	w_2	h	t	Feed Pos
For Frequency (MHz)	915	12.8	0.9	0.1	12.5	2.5	1.0	4.0
	2450	7.5	0.64	0.15	6.0	2.5	1.29	1.5

MHz and 2450 MHz, respectively.

II. ANTENNA GEOMETRY

The starting point of the antenna development was the vertical loop presented in [2], where the antenna was shown to provide a compelling size-performance balance for a miniature radio-frequency identification (RFID) tag mountable directly on metallic items. Similarly, implantable antennas need to be electrically small and capable of functioning in an unwelcoming environment formed by the lossy biological tissue.

To design the proposed antenna, we construct a seven-layered elliptical model to mimic the head phantom, as shown in Fig. 1(a). The structure and dimensional parameters of the proposed antenna are depicted in Fig. 1(b).

The resonance of the studied antenna is primarily controlled by the length; however, the thickness and width of this antenna can be thinner to control the overall geometry. In further steps, the loop is excited from the central layer, and a third top layer is added to be capacitively coupled to provide impedance matching and lower the resonance frequency. A substrate RO3210 ($\epsilon_r = 10.2$ and $\tan \delta = 0.003$), with a thickness of 0.9 mm, has been used as the first layer substrate, and PDMS ($\epsilon_r = 2.2$ and $\tan \delta = 0.007$), with a thickness of 0.1 mm, is used as the top layer substrate as well as for coating of the antenna. To connect the ends of the layers, vias are used to form a G-shaped geometry with the isolated far ends.

III. RESULTS AND DISCUSSION

To design the proposed antennas, as shown in Fig. 1(a), a seven-layer simulation setup was made in ANSYS high-frequency structure simulator (HFSS). Firstly, the antenna was modified in a couple of steps from the vertical loop antenna and its initial fundamental resonance frequency was around 1.5 GHz. The proposed antennas were then optimized through a series of parametric analyses, which are discussed as follows:

A. Parametric studies

To achieve the required resonances at 915 MHz and 2450 MHz, different dimensional parameters of the proposed antenna have been studied to see the relationship between the specific parameters and the resonance of the antenna.

Fig. 2 shows the relationship of the resonance to changes in the thickness of the layers and the width of the antenna. Fig. 2(a) shows that keeping the thickness of layer-2 (h_2) at 0.1 mm and increasing the thickness of layer-1 (h_1) in the range 0.5–0.9 mm, shifts the resonance to a lower range from 1.45 GHz to 1.25 GHz. This shift in resonance is due to the increase in (h_1) lengthens the vias, which stretches the overall length. On the other hand, keeping h_2 at 0.4 mm and increasing (h_1) in

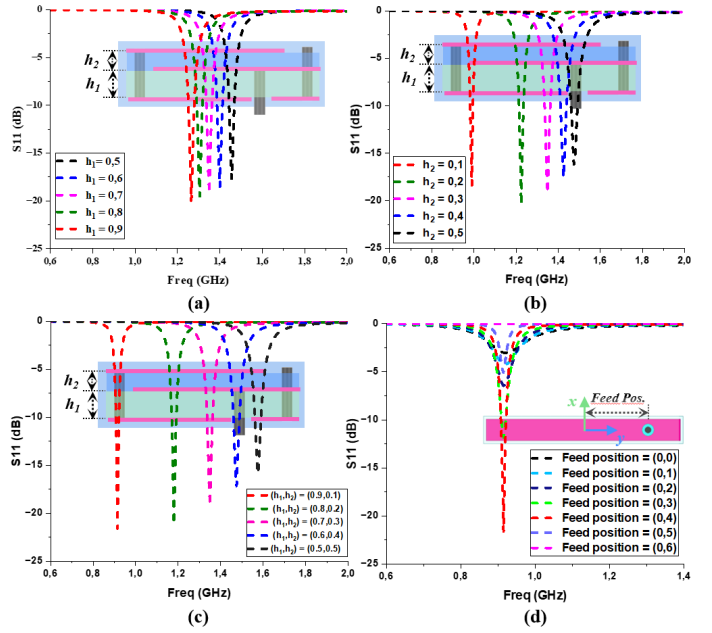


Fig. 2. Effects of the thicknesses of the substrate layers' widths and Feed position of the antenna on its resonance frequency. (a) Resonance v/s h_1 . (b) Resonance v/s h_2 . (c) Combining effects of h_1 and h_2 on the resonance. (d) Effects of the Feed position on the resonance of the antenna.

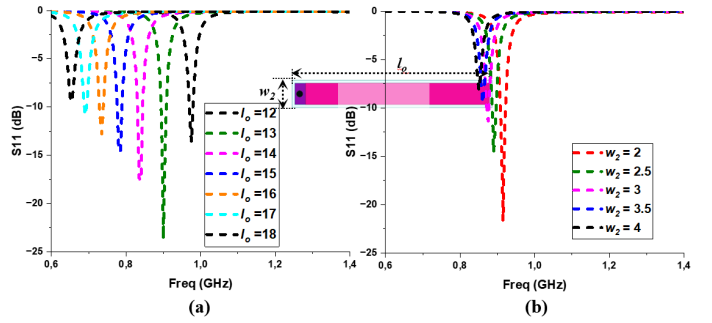


Fig. 3. Effects of changing length and width of the proposed antenna. (a) Effects of length on the resonance of the antenna. (b) Effects of width on the resonance of the antenna.

the range of 0.1–0.5 mm, the resonance of the antenna shifts to higher (from 1.0 GHz to 1.8 GHz), as shown in Fig. 2(b). This increase in the resonance frequency due to an increase in the thicknesses of the substrates is because the thickness of the top layer substrate h_1 plays an important role in the capacitive coupling between the top layer and middle layer of the antenna, and decreasing the thickness of the top layer substrate decreases this coupling.

Based on the conclusion of the analysis mentioned above, we studied the combining effects of h_1 and h_2 in Fig. 2(c) to quantify the tolerance limits of resonance shift due to the thicknesses of the substrates. Therefore, we kept the overall thickness of the substrate layers (h) to 1 mm ($h = h_1 + h_2 = 1$ mm) and evaluated the performance of the antenna by changing the thickness of the substrates properly. As a result decreasing h_2 and increasing h_1 , the resonance can be tuned

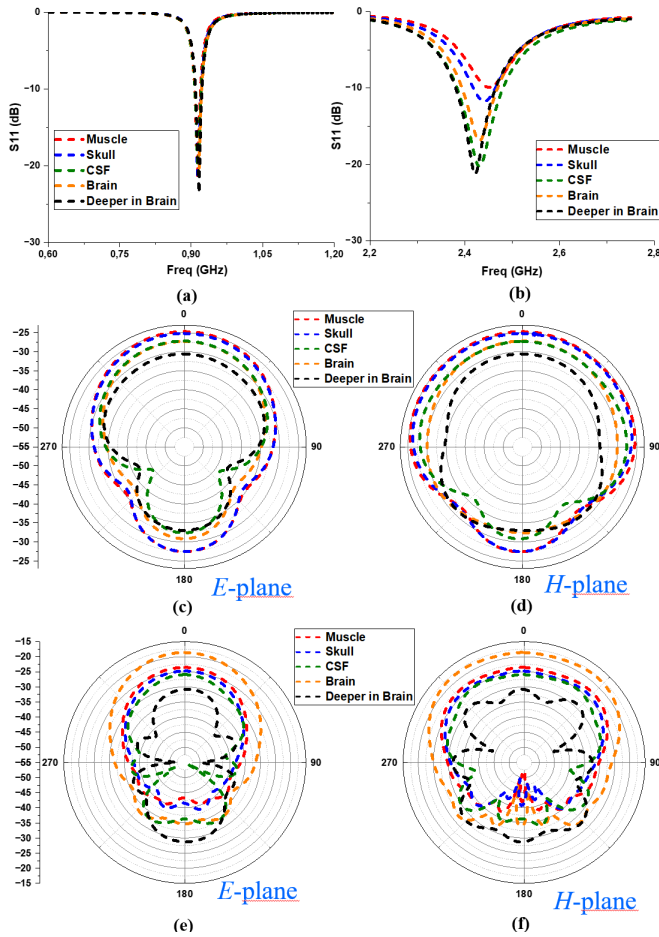


Fig. 4. S-parameters and radiation patterns at different implantation depths. (a) S-parameters of the 915 MHz antenna. (b) S-parameters of the 2450 MHz antenna. (c), (d) E and H -planes of gain patterns of 915 MHz antenna. (e), (f) E and H -planes of gain patterns of 2450 MHz antenna.

to around 900 MHz. To achieve better impedance matching, the Feed position is moved across the length of the antenna Fig. 2(d), respectively. The feed position solely controls the impedance matching, and improves it as the feed moves away from the center toward the connected edge of the antenna. This enhancement in the impedance matching is due to the increase of coupling of feed with the vias, which increases the inductance of the antenna to conjugate the capacitance.

To further reduce the size of the antenna, its length (l_o), and width (w_2) have been parametrically analyzed. As shown in Fig. 3(a) the analysis revealed that by changing the length, the frequency tolerance of 500 MHz can be compensated with length and this antenna can be optimized to be operated at different frequencies such as 402, 915, and 2450 MHz. In contrast, the antenna's width significantly controls its impedance matching, as depicted in Fig. 3(b). It is evident from the figure that the narrower width leads to good impedance matching. This enhancement in impedance matching is due to decreased capacitive coupled area and increased inductance by accelerating the currents through narrow paths. Additionally, due increase in the inductance of the antenna, its resonance shifts

to lower frequencies.

Based on the above scalability analysis, it is evident that this antenna can be easily optimized at different frequencies by changing the length, width, and thickness of its layers. Hence, we developed its two samples: at 915 MHz and 2450 GHz. The optimized geometric parameters' values are presented in Table 1, where the length of the antenna operating at 915 MHz is 12.8 mm and for 2450 MHz is 7.5 mm, respectively.

Interestingly, unlike previous antennas whose radiation patterns are detuned and distorted by implantation depth, this antenna maintains its performance regardless of how deep it is implanted. For the proof of concept, the analysis of both (915 and 2450 MHz) antennas at different implantation depths is presented in Fig. 4. Fig. 4(a) and (b) depict the S-parameters of the 915 and 2450 MHz antennas implanted at different depths. It is clear from the figure that the resonance of this antenna at 915 MHz is less sensitive to implantation depth and dielectric environment. However, a small deviation in the resonance of the 2450 MHz antenna is noticed when the implantation depth is varied.

Figures 4(c) and (d) present the E and H -planes of radiation patterns of the 915 MHz antenna, where the peak value decreases with implantation depth. However, the overall shape of the radiation pattern does not change with implantation depth. Conversely, at different implantation depths, the radiation pattern of the 2450 MHz antenna follows the same trend but also shows a minute deviation in the shape of the pattern as the depth increases. Nevertheless, this deviation in resonance and pattern shape can be minimized by exploring the relationship between parameterizing the geometrical dimensions of the 2450 MHz antenna and implantation depth. Additionally, the medium unaffected dipole-like radiation pattern of 915 MHz and wide beam-width of 2450 MHz antenna make these antennas suitable for efficient I2I communication.

IV. CONCLUSION

We presented an environment-unaffected implantable antenna in a seven-layer head phantom. For scalability, its geometry is parametrically analyzed, and based on these analyses two antennas' geometries (915 and 2450 MHz antennas) were optimized. Further, the radiation patterns and resonances of these antennas were studied at different implantation depths, where the antennas showed stable performance. The fractional bandwidths of 3.1% and 15% successfully cover the ISM frequency bands centered at 915 MHz and 2450 MHz. Given the wide beamwidths, high efficiencies and gains, and environment-unaffected performance of these antennas, we anticipate significant advancements in I2I communication in the future.

REFERENCES

- [1] A. Basir et al., "Implantable and ingestible antenna systems: From imagination to realization [bioelectromagnetics]," *IEEE Antennas Propag. Mag.*, vol. 65, no. 5, pp. 70–83, Oct. 2023.
- [2] K. Jaakkola, "Small on-metal UHF RFID transponder with long read range," *IEEE Trans. Antennas Propag.*, vol. 64, no. 11, pp. 4859–4867, Nov. 2016.